Trop J Nat Prod Res, March 2025; 9(3): 1105 - 1111 **ISSN 2616-0684 (Print)**
ISSN 2616-0692 (Electronic)

Tropical Journal of Natural Product Research

Available online at https://www.tjnpr.org

Original Research Article

α-Glucosidase and xanthine oxidase inhibitory activities from the fruits of Thai *Averrhoa bilimbi* L.

Thuy T. L. Nguyen[1], Thanh Q. Tran[2], Lien T. M. Do[3], Nhat M. Huynh[3], Kewalin Inthanon[4], Jirapast Sichaem[4]*

[1]*Department of Biotechnology, Ho Chi Minh City Open University, Ho Chi Minh City 712006, Vietnam*
[2]*University of Science, National University – Ho Chi Minh City, Ho Chi Minh City 748500, Vietnam*
[3]*Sai Gon University, Ho Chi Minh City 748000, Vietnam*
[4]*Research Unit in Natural Products Chemistry and Bioactivities, Faculty of Science and Technology, Thammasat University Lampang Campus, Lampang 52190, Thailand.*

ARTICLE INFO

Article history:
Received 14 December 2024
Revised 31 December 2024
Accepted 07 January 2025
Published online 01 April 2025

Copyright: © 2025 Nguyen *et al*. This is an open-access article distributed under the terms of the Creative Commons Attribution License, which permits unrestricted use, distribution, and reproduction in any medium, provided the original author and source are credited.

ABSTRACT

Averrhoa bilimbi L., a tropical plant native to Southeast Asia, is traditionally used in folk medicine to treat various ailments, including infections, inflammation, hypertension, obesity, and diabetes. In this study, the fruits of *A. bilimbi* L. were successfully isolated and identified as β-sitosterol **(**1), zeorin **(**2**),** helilandin B (3**),** 2′-hydroxy-3′,4′,6′-trimethoxychalcone **(**4), myricetin (5), quercetin (6), cinchonain Ia (7), syringaresinol (8), and syringaresinol diglucoside (9). All the isolated compounds were tested for their inhibitory effects on α-glucosidase and xanthine oxidase (XO) activities. Compounds 3 and 4 demonstrated the strongest α-glucosidase inhibitory activity, with IC_{50} values of 4.10 ± 0.20 and 4.79 ± 0.27 μM, respectively. Compound 4 exhibited the highest XO inhibition, with an IC_{50} value of 48.4 ± 0.03 μM. These findings highlight the potential of the bioactive compounds from *A. bilimbi* L. as promising candidates for therapeutic applications in the management of diabetes and hyperuricemia.

Keywords: Oxalidaceae, *Averrhoa bilimbi* L., Phytochemical constituents, α-Glucosidase inhibition, Xanthine oxidase inhibition.

Introduction

Averrhoa bilimbi L., a perennial plant in the Oxalidaceae family, is native to tropical Southeast Asia. Traditionally, the leaves are used in infusions and decoctions to manage fever, rectal inflammation, diabetes, and postpartum health.[1] Additionally, leaf paste is applied for skin conditions like itching, boils, and eruptions, as well as for rheumatism, colds, mumps, syphilis, and venomous animal bites.[2] Its fruits and flowers are also used in folk medicine to treat a variety of ailments, including thrush, fever, inflammation, rectal bleeding, hemorrhoids,[3] whooping cough, acne, hypertension, obesity, and diabetes.[4] Previous reports highlight the medicinal properties of *A. bilimbi* L., including antimicrobial,[4] antioxidant,[5] anti-inflammatory,[6] wound-healing,[7] analgesic,[8] muscle-relaxant,[9] hepatoprotective,[10] antihypertensive,[11] anticancer,[12] and antidiabetic[13] activities. Phytochemical analyses have identified various bioactive compounds in *A. bilimbi* L., including phenols, flavonoids, triterpenoids, anthocyanins, alkaloids, saponins, coumarins, tannins, phytosterols, and cardiac glycosides.[14] Although some specific compounds have been isolated from *A. bilimbi* L.,[15,16] studies directly linking these compounds to pharmacological activities remain limited.

*Corresponding author. Email: jirapast@tu.ac.th
Tel: +66 54237999

Citation: Nguyen TTL, Tran TQ, Do LTM, Huynh NM, Inthanon K, Sichaem J. α-Glucosidase and xanthine oxidase inhibitory activities from the fruits of Thai *Averrhoa bilimbi* L. Trop J Nat Prod Res. 2025; 9(3): 1105 - 1111 https://doi.org/10.26538/tjnpr/v9i3.27

Official Journal of Natural Product Research Group, Faculty of Pharmacy, University of Benin, Benin City, Nigeria

The inhibition of α-glucosidase and xanthine oxidase (XO) enzymes represents a promising therapeutic strategy for managing type 2 diabetes and hyperuricemia, respectively.[17] α-Glucosidase, a key enzyme involved in carbohydrate digestion, catalyzes the breakdown of complex carbohydrates into glucose, thereby playing a pivotal role in the management of postprandial hyperglycemia.[18] Conversely, XO is essential in purine metabolism and the production of uric acid, making its inhibition an effective strategy for controlling gout and related conditions.[19] The potential of natural compounds to inhibit these enzymes presents an attractive opportunity for developing bioactive agents with fewer side effects compared to synthetic inhibitors.[20] As part of our ongoing research to identify α-glucosidase and xanthine oxidase inhibitors from Thai medicinal plants,[13,21,22] we have isolated and elucidated nine compounds (1–9) from the fruits of *A. bilimbi* L. (Figure 1). The α-glucosidase and xanthine oxidase inhibitory activities of all isolated compounds were assayed.

Materials and Method

General experimental procedures

Column chromatography was carried out using silica gel 60 (particle size 0.040–0.063 mm, Silicycle) and Sephadex LH-20 (GE Healthcare Bio-Sciences AB, Uppsala, Sweden). Thin-layer chromatography (TLC) was utilized to monitor fractions and isolated compounds, employing silica gel 60 F_{254} plates (Merck). Nuclear magnetic resonance (NMR) spectra were recorded using Bruker AvanceNEO 600 and Bruker Avance 500 spectrometers. High-resolution electrospray ionization mass spectrometry (HRESIMS) was performed using an X500R QTOF mass spectrometer (Sciex, USA) and a Dionex Ultimate 3000 HPLC system paired with a QExactive Hybrid Quadrupole Orbitrap mass spectrometer (Thermo Fisher Scientific).

Plant material

The fruits of *Averrhoa bilimbi* L. were harvested in October 2023 from Uttaradit Province, Thailand. The plant was verified and authenticated by Asst. Prof. Dr. Kanit Wangwasit from the Department of Biology,

© 2025 the authors. This work is licensed under the Creative Commons Attribution 4.0 International License

Faculty of Science, Mahasarakham University, Thailand, where a voucher specimen (K. Wangwasit 240807-1) was maintained.

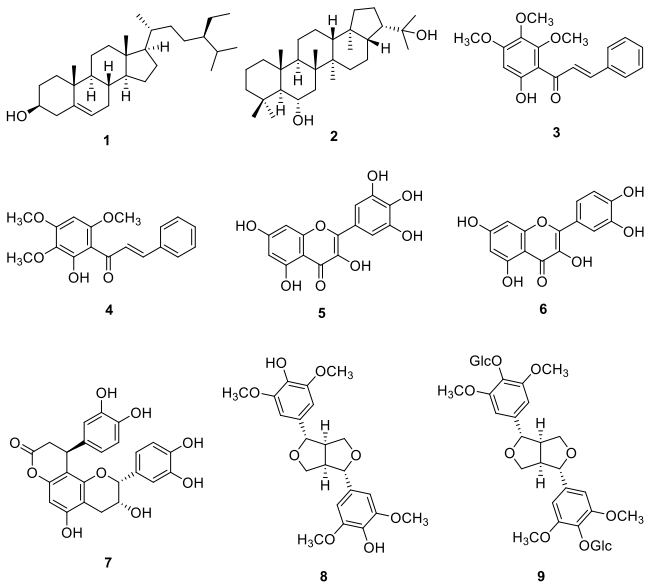

Figure 1. Chemical structures of **1**-**9**.

Extraction and isolation

The dried powder of *A. bilimbi* L. fruits (1.7 kg) was extensively extracted at room temperature using 95% ethanol (EtOH) (6 L × 5). The combined EtOH extracts were concentrated under reduced pressure to obtain a crude residue (111.5 g). This crude EtOH extract was dissolved in water and partitioned successively with *n*-hexane and ethyl acetate (EtOAc), yielding *n*-hexane (42.0 g) and EtOAc (28.0 g) fractions. The EtOAc fraction was subjected to silica gel column chromatography (CC) with gradient elution using *n*-hexane–EtOAc (8:2 to 0:10, *v*/*v*) and EtOAc–methanol (MeOH) (10:0 to 0:10, *v*/*v*). Based on thin-layer chromatography (TLC) profiles, the eluates were combined into eight fractions (EA.1–EA.8). Fraction EA.2 (1.4 g) underwent further separation on silica gel CC eluted with *n*-hexane–EtOAc (8:2, *v*/*v*), yielding in five subfractions (EA.2.1–EA.2.5). Subfraction EA.2.2 (0.2 g) was purified through silica gel CC with *n*-hexane–EtOAc (8:2, *v*/*v*), followed by Sephadex LH-20 CC using chloroform ($CHCl_3$)–MeOH (1:4, *v*/*v*), affording **1** (16.7 mg) and **2** (3.8 mg). Similarly, subfraction EA.2.3 (0.4 g) was purified to yield **3** (4.5 mg) and **4** (5.2 mg). Fraction EA.3 (1.5 g) was fractionated on silica gel CC eluted with *n*-hexane–EtOAc (75:25, *v*/*v*), producing four subfractions (EA.3.1–EA.3.4). Compound **8** (12.0 mg) was obtained from subfraction EA.3.1 (0.3 g) after further purification through silica gel CC eluted with *n*-hexane–EtOAc (75:25, *v*/*v*) and Sephadex LH-20 CC using $CHCl_3$–MeOH (1:4, *v*/*v*). Fraction EA.5 (3.5 g) was separated on silica gel CC with *n*-hexane–EtOAc (7:3, *v*/*v*), resulting in seven subfractions (EA.5.1–EA.5.7). From subfraction EA.5.2 (0.3 g), compounds **5** (7.5 mg) and **6** (8.5 mg) were purified using silica gel CC with $CHCl_3$–MeOH (95:5, *v*/*v*), followed by Sephadex LH-20 CC with $CHCl_3$–MeOH (1:4, *v*/*v*). Compound **7** (8.0 mg) was isolated from subfraction EA.5.4 (0.4 g) using the same chromatographic techniques. Fraction EA.7 (4.5 g) was fractionated on silica gel CC eluted with *n*-hexane–EtOAc (6:4, *v*/*v*), yielding seven subfractions (EA.7.1–EA.7.7). Subfraction EA.7.2 (0.4 g) was further purified through silica gel CC with $CHCl_3$–MeOH (9:1, *v*/*v*) and Sephadex LH-20 CC using $CHCl_3$–MeOH (1:4, *v*/*v*), resulting in the isolation of **9** (6.5 mg).

α-Glucosidase inhibition assay

The *α*-glucosidase inhibition assay was conducted following a previously established method[22] with slight modifications. Solution A was prepared by dissolving yeast *α*-glucosidase (0.1 U/mL) and *p*-nitrophenyl-*α*-D-glucopyranoside (1 mM) in a 0.1 M phosphate buffer at pH 6.9. For Solution B, 10 μL of the test sample was mixed with 40 μL of *α*-glucosidase solution and incubated at 37℃ for 10 min. The reaction was initiated by adding 50 μL of Solution A to Solution B, followed by another incubation at 37°C for 20 min. To stop the reaction, 100 μL of 1 M Na_2CO_3 was added. Absorbance was recorded at 405 nm, and the percentage of inhibition was determined using the following formula $[(A_0 - A_1) / A_0] \times 100$, where A_0 represents the absorbance of the control (no sample), and A_1 is the absorbance with the sample. The IC_{50} value (the concentration of inhibitor required to reduce enzyme activity by 50%) was determined from a concentration-inhibition curve. All experiments were conducted in triplicate, and the results were presented as mean ± standard deviation. The inhibitory activity of the samples was compared to acarbose, which was used as a positive control.

Xanthine oxidase inhibition assay

The test samples were initially prepared as 10 mM stock solutions in dimethyl sulfoxide (DMSO) and subsequently diluted with phosphate buffer to achieve the desired concentrations. The assay for xanthine oxidase (XO) inhibition utilized xanthine as a substrate, following a previously established protocol.[23] Briefly, 100 μL of xanthine oxidase solution (0.03 U/mL) in 50 mM phosphate buffer (pH 7.5) was combined with 50 μL of the test sample in a 96-well plate. After a 5-minute incubation at 37 ℃, 50 μL of xanthine solution (0.60 mM) was added to initiate the reaction. The reaction progress was monitored by measuring the absorbance at 295 nm every minute for 10 min using a microplate reader. The phosphate buffer was used as the vehicle control, while allopurinol served as the positive control. The XO inhibitory activity was assessed by comparing the absorbance of the test samples to those of the control wells. The IC_{50} value was determined using GraphPad Prism 8.0 software.

Results and Discussion

Phytochemical identification

The phytochemical investigation of Thai *A. bilimbi* L. fruits using chromatographic and spectroscopic techniques led to the identification of nine compounds, including *β*-sitosterol (**1**), zeorin (**2**), helilandin B (**3**), 2′-hydroxy-3′,4′,6′-trimethoxychalcone (**4**), myricetin (**5**), quercetin (**6**), cinchonain Ia (**7**), syringaresinol (**8**), and syringaresinol diglucoside (**9**). Their chemical structures were elucidated through extensive spectroscopic methods and comparisons with those previously reported. Compound **1** was characterized as a white crystal. Analysis of the ^1H and ^{13}C NMR data (Table 1) revealed that it belongs to the class of sterol-type compounds. Its ^1H NMR data displayed a multiplet at δ_H 5.35, corresponding to an olefinic proton, and a triplet of doublets of doublets at δ_H 3.52, attributed to a carbinolic proton. The ^{13}C NMR data revealed one olefinic methine carbon (δ_C 141.0), indicative of a carbon-carbon double bond. Based on its NMR spectral data and a comparison with previous literature, compound **1** was assigned as *β*-sitosterol, a commonly occurring plant-derived sterol.[24] Compound **2** was obtained as a colorless solid. Analysis of the ^1H and ^{13}C NMR data (Table 1) indicated that it belongs to the class of hopane-type triterpenes. The upfield methine proton H-5 (δ_H 0.72, d, J = 10.8 Hz) displayed a 1,2-diaxial coupling with the oxymethine proton (δ_H 3.75, ddd, J = 10.2, 6.0, 4.2 Hz), indicating that the hydroxyl group at C-6 was oriented in the *α*-configuration. The key signal for the identification of the 6-OH group of **2** was also determined through analysis of the HMBC data. Based on the above data, compound **2** was determined as zeorin.[25]

Compound **3** was isolated as a yellow wax. The ^1H NMR data of **3** (Table 2) revealed signals characteristic of a hydrogen-bonded hydroxyl proton (δ_H 12.18), a pair of *trans* olefinic protons at δ_H 7.61 (d, J = 15.6 Hz) and 7.58 (d, J = 15.6 Hz), a phenyl group at δ_H 7.72 (m) and 7.45 (m), a singlet aromatic proton (δ_H 6.39), and three singlet methoxyl protons at δ_H 3.84 (× 2) and 3.70. The analysis of the ^{13}C NMR spectrum exhibited 18 signals, including one ketone carbonyl (δ_C 193.0) and four oxygenated aromatic (δ_C 162.7, 160.2, 155.0, and 135.4) carbons. The positions of the methoxy groups at C-4′, C-5′, and C-6′ were confirmed through HMBC correlations. Based on this spectral analysis, compound **3** was identified as a chalcone derivative, named helilandin B.[26]

Compound **4** was characterized as yellow wax.

© 2025 the authors. This work is licensed under the Creative Commons Attribution 4.0 International License

Table 1: ^{1}H (600 MHz) and ^{13}C (150 MHz) NMR data of **1** and **2** in DMSO-d_6 (δ in ppm, J in Hz)

No.	1		2	
	δ_H	δ_C	δ_H	δ_C
1		37.4		40.9
2		31.8		18.0
3	3.52 (tdd, 4.8, 4.2, 3.6)	72.0		43.6
4		42.4		33.3
5		141.0	0.72 (d, 10.8)	59.9
6	5.35 (m)	122.0	3.75 (ddd, 10.2, 6.0, 4.2)	66.6
7		32.1	1.93 (d, 13.2)	44.7
			1.35 (d, 3.5)	
8		32.0		42.1
9		50.3		49.3
10		36.6		38.6
11		21.2		21.3
12		39.9		23.6
13		42.5		48.9
14		56.9		41.4
15		26.2		33.9
16		28.4		20.6
17		56.2		53.8
18	0.68 (s)	18.9		43.6
19	1.01 (s)	12.0		40.9
20		36.3		26.1
21	0.92 (d, 6.6)	19.2	2.09 (m)	50.4
22		34.1		71.5
23		24.5	1.12 (s)	36.6
24		46.0	0.94 (s)	21.9
25		29.3	0.81 (s)	16.8
26	0.83 (d, 6.6)	20.0	0.98 (s)	18.1
27	0.81 (d, 6.6)	19.6	0.92 (s)	16.9
28		23.2	0.71 (s)	15.8
29	0.84 (t, 7.2)	12.1	1.03 (s)	28.9
30			1.07 (s)	30.8
6-OH			3.88 (d, 6.6)	
22-OH			3.81 (s)	

© 2025 the authors. This work is licensed under the Creative Commons Attribution 4.0 International License

Table 2: ^{1}H (600 MHz) and ^{13}C (150 MHz) NMR data of **3**, **4**, **8**, and **9** in DMSO-d_6 (δ in ppm, J in Hz)

No.	3		4		8		9	
	δ_H	δ_C	δ_H	δ_C	δ_H	δ_C	δ_H	δ_C
1		135.3		134.7		131.5		137.1
2	7.72 (m)	128.4	7.72 (m)	128.4	6.60 (s)	103.7	6.66 (s)	105.0
3	7.45 (m)	129.0	7.46 (m)	129.0		147.9		152.6
4	7.45 (m)	130.3	7.46 (m)	130.5		134.9		134.1
5	7.45 (m)	129.0	7.46 (m)	128.4		147.9		152.6
6	7.72 (m)	128.4	7.72 (m)	129.0	6.60 (s)	103.7	6.66 (s)	105.0
7		193.0		192.8	4.62 (d, 4.2)	85.3	4.67 (d, 3.6)	85.0
8	7.61 (d, 15.6)	126.6	7.68 (d, 15.6)	127.6	3.06 (m)	53.7	3.46 (m)	53.7
9	7.58 (d, 15.6)	143.2	7.61 (d, 15.6)	142.5	4.17 (m)	71.1	3.82 (m)	67.3
					4.16 (m)		4.20 (m)	
1′		108.8		107.1		131.5		137.1
2′		162.7		155.7	6.60 (s)	103.7	6.66 (s)	105.0
3′	6.39 (s)	96.6	6.11(d, 2.5)	130.5		147.9		152.6
4′		155.0		157.7		134.9		134.1
5′		135.4	6.30 (s)	88.5		147.9		152.6
6′		160.2		157.3	6.60 (s)	103.7	6.66 (s)	105.0
7′					4.62 (d, 4.2)	85.3	4.67 (d, 3.6)	85.0
8′					3.06 (m)	53.7	3.46 (m)	53.7
9′					4.17 (m)	71.1	3.82 (m)	67.3
					4.16 (m)		4.20 (m)	
1″							5.15 (d, 7.2)	101.3
2″							3.46 (m)	71.3
3″							3.42 (m)	71.3
4″							3.36 (m)	70.5
5″							3.20 (m)	75.2
6″							3.43 (m)	61.2
							3.57 (m)	
3,5-OCH_3					3.77 (s)	56.0	3.85 (s)	56.4
3′-OCH_3			3.65 (s)	60.0	3.77 (s)	56.0	3.84 (s)	56.4
4′-OCH_3	3.70 (s)	60.6	3.92 (s)	56.1				
5′-OCH_3	3.84 (s)	61.5			3.77 (s)	56.0	3.84 (s)	56.4
6′-OCH_3	3.84 (s)	56.1	3.92 (s)	56.0				
4,4′-OH					8.24 (s)			
2′-OH	12.18 (s)		12.63 (s)					

A detailed analysis of the ^{1}H and ^{13}C NMR data of **4** (Table 2) revealed a structure closely resembling that of **3**, with one key difference. In **4**, a methoxy group was located at C-3′ and a methine proton at C-5′, whereas in **3**, these positions were reversed, with a methoxy group at C-5′ and a methine proton at C-3′. The HMBC correlations confirmed the precise placement of all substituents on ring A. Based on this analysis, the structure of **4** was determined as 2′-hydroxy-3′,4′,6′-trimethoxychalcone.[27] Compound **5** was obtained as a pale yellow powder. The ^{1}H NMR data of **5** (Table 3) revealed two doublet signals

© 2025 the authors. This work is licensed under the Creative Commons Attribution 4.0 International License

at δ_H 6.37 (d, J = 2.4 Hz) and δ_H 6.18 (d, J = 1.8 Hz), corresponding to two *meta*-coupled protons of ring A. A singlet signal at δ_H 7.23 (× 2) was observed, corresponding to two symmetrical protons on ring B. Additionally, singlet signals for six hydroxyl groups were observed at δ_H 12.48, 10.79, 9.31, 9.21 (× 2), and 8.78. The HMBC correlations confirmed the positions of these hydroxyl groups at C-3 (δ_C 135.9), C-5 (δ_C 160.7), C-3′ (δ_C 145.7), C-4′ (δ_C 135.9), and C-5′ (δ_C 145.7). Accordingly, compound **5** was identified as a flavonol known as myricetin.[28]

Table 3: ^{1}H (600 MHz) and ^{13}C (150 MHz) NMR data of **5-7** in DMSO-d_6 (δ in ppm, J in Hz)

No.	5		6		7	
	δ_H	δ_C	δ_H	δ_C	δ_H	δ_C
2		146.8		146.8	4.84 (s)	78.4
3		135.8		135.7	4.09 (d, 3.0)	64.2
4		175.7		175.8	2.78 (dd, 16.8, 4.2)	28.3
					2.56 (dd, 17.4, 3.6)	
5		160.7		160.7		155.4
6	6.18 (d, 1.8)	98.1	6.18 (d, 1.8)	98.1	6.20 (s)	94.9
7		163.8		163.8		151.9
8	6.37 (d, 2.4)	93.2	6.40 (d, 1.8)	93.3		104.1
9		156.1		156.1		150.1
10		103.0		103.0		104.1
1′		120.8		121.9		130.0
2′	7.23 (s)	107.2	7.67 (d, 2.4)	115.0	6.79 (d, 1.8)	114.4
3′		145.7		145.0		143.9
4′		135.9		147.6		144.4
5′		145.7	6.88 (d, 8.4)	115.5	6.63 (d, 7.8)	115.6
6′	7.23 (s)	107.2	7.54 (dd, 8.4, 2.4)	119.9	6.48 (dd, 8.4, 1.8)	117.8
α					3.08 (dd, 15.6, 7.2)	37.4
					2.71 (dd, 15.6, 1.2)	
β					4.31 (d, 6.6)	33.2
1″						133.2
2″					6.49 (d, 1.8)	114.7
3″						144.5
4″						145.1
5″					6.57 (d, 8.4)	115.6
6″					6.42 (d, 8.4, 1.8)	117.7
-COO-						168.1
3-OH	9.31 (s)		9.32(s)		4.66 (d, 4.2)	
5-OH	12.48 (s)		12.48 (s)		9.66 (s)	
7-OH	10.79 (s)		10.75 (s)			
3′-OH	9.21 (s)		9.27 (s)		8.74 (s)	
4′-OH	8.78 (s)		9.55 (s)		8.70 (s)	
5′-OH	9.21 (s)					
3″-OH					8.74 (s)	
4″-OH					8.65 (s)	

© 2025 the authors. This work is licensed under the Creative Commons Attribution 4.0 International License

Compound **6** was isolated as a pale yellow powder. Analysis of the ^{1}H and ^{13}C NMR data (Table 3) revealed the characteristics of a flavonol skeleton, similar to those of **5**. The NMR data differed in the presence of a methine proton at δ_H 6.88 (d, J = 8.4 Hz) instead of a hydroxyl group at C-5′ (δ_C 115.5) on ring B. Consistent with this observation, compound **6** was determined as quercetin, a pigment found in many plants.[29] Compound **7** was obtained as yellow wax. The ^{1}H NMR data (Table 3) indicated the presence of a flavan-3-ol framework, as evidenced by AMX$_2$-type signals at δ_H 4.84 (s), 4.09 (d, J = 3.0 Hz), 2.78 (dd, J = 16.8, 4.2 Hz), and 2.56 (dd, J = 17.4, 3.6 Hz), corresponding to H-2, H-3, and H-4, respectively. A singlet aromatic proton signal at δ_H 6.20 suggested a trisubstituted A-ring. The aromatic ABX-type signals at δ_H 6.79 (d, J = 1.8 Hz), 6.63 (d, J = 7.8 Hz), and 6.48 (dd, J = 8.4, 1.8 Hz), along with the chemical shifts and coupling patterns, confirmed the presence of a 5,7,3′,4′-tetrahydroxyflavan-3-ol core. The substituent was identified through ^{1}H and ^{13}C NMR analysis, revealing mutually coupled benzylic methine signals at δ_H 4.31 (d, J = 6.6 Hz) and methylene signals at δ_H 3.08 (dd, J = 15.6, 7.2 Hz) and 2.71 (dd, J = 15.6, 1.2 Hz). Additional ABX-type aromatic signals at δ_H 6.57 (d, J = 8.4 Hz), 6.49 (d, J = 1.8 Hz), and 6.42 (dd, J = 8.4, 1.8 Hz), along with a carboxyl carbon signal at δ_C 168.1, were also observed. These findings suggested the presence of a phenylpropanoid (C_6–C_3) unit containing a 3,4-dihydroxy aromatic system, linked to the benzylic β-position *via* a carbon–carbon bond. Thus, compound **7** was identified as cinchonain Ia.[30]

Compound **8** was characterized as a white wax. The ^{1}H and ^{13}C NMR data of **8** (Table 2) displayed singlet signals for four aromatic protons at δ_H 6.60 × 4, two hydroxyl groups at δ_H 8.24 × 2, four methoxy groups at δ_H 3.77 × 4, and signals corresponding to a 3,7-dioxabicyclo[3.3.0] octane-type lignan with eight aliphatic protons. The simplicity of the ^{1}H and ^{13}C NMR spectra suggested that 8 is a symmetrical lignan. Stereochemically, the bicyclooctane-type lignans were determined to occur naturally in the *cis*-configuration of the protons, based on the coupling constants between H-7/H-7′ and H-8/H-8′. Accordingly, the structure of 8 was assigned as syringaresinol.[31] Compound 9 was isolated as a white wax. Analysis of the ^{1}H and ^{13}C NMR data of 9 (Table 2) revealed similarities to those of 8, with the notable exception of two β–D-glucopyranosyl moieties located at C-4 and C-4′. The presence of these sugar moieties was confirmed through HMBC networks. Based on this analysis, the structure of 9 was identified as a symmetrical lignan glycoside, named syringaresinol diglucoside.[32]

Bioactivities

The α-glucosidase inhibitory activity of **1-9** was assessed (Table 4). Among them, compounds **3** and **4** showed the strongest inhibitory effects, with IC$_{50}$ values of 4.10 ± 0.20 and 4.79 ± 0.27 μM, respectively. These values indicate significantly greater activity compared to the positive control, acarbose (IC$_{50}$ 170 ± 4.12 μM), emphasizing their potential for further research and development. The other compounds, except for compound **1**, exhibited good inhibition, with IC$_{50}$ values in the range of 17.6–82.3 μM, while compound **1** displayed no significant activity (>250 μM). Although the structures of the isolated compounds varied significantly, including steroid, triterpenoid, chalcones, flavonolignan, flavonoids, and lignans, chalcones (**3** and **4**) exhibited the most potent α-glucosidase inhibition. These compounds demonstrated approximately 40-fold stronger inhibitory activity against α-glucosidase compared to the standard acarbose. This result is consistent with previous findings, which suggest that the presence of a 2′-hydroxyl group on ring B, along with the structural flexibility of chalcones, enhances their inhibitory activity.[33] These features play a crucial role in the interaction of chalcones (**3** and **4**) with the enzyme. Although some studies have reported that chalcones and their derivatives can inhibit α-glucosidase, research investigating the inhibitory effects of chalcones on this enzyme remains limited.[34]

All isolated compounds were also tested for their XO inhibitory activity (Table 4). Compounds **4** and **7** displayed XO inhibition, with IC$_{50}$ values of 48.4 ± 0.03 and 52.8 ± 0.02 μM, respectively. Other compounds displayed IC$_{50}$ values >100 μM, indicating no significant inhibition. Notably, among the two isolated chalcones (**3** and **4**), compound **4** demonstrated the highest activity (IC$_{50}$ value of 48.4 ± 0.03 μM), whereas **3** was completely inactive. The potent activity of **4** could be linked to the placement of methoxy groups at positions C-3, C-4, and C-6 on the A-ring. To date, only a limited number of studies have reported the XO inhibitory activity of flavonolignans.[35,36] Based on the IC$_{50}$ value of **7** (52.8 ± 0.02 μM), these findings further support the XO inhibitory potential of this class of flavonolignans. These results suggest that chalcone (**4**) and flavonolignan (**7**) are bioactive constituents of *A. bilimbi* L., with significant potential for use in gout treatment.

Table 4: α-Glucosidase and xanthine oxidase inhibitory activities of 1-9

Compound	IC$_{50}$ (μM)[a]	
	α-Glucosidase	Xanthine oxidase
1	>250	ND[b]
2	64.1 ± 2.14	>100
3	4.10 ± 0.20	>100
4	4.79 ± 0.27	48.4 ± 0.03
5	62.3 ± 1.17	>100
6	51.1 ± 1.37	>100
7	17.6 ± 0.45	52.8 ± 0.02
8	82.3 ± 2.75	>100
9	44.2 ± 0.74	>100
Acarbose[c]	170 ± 4.12	
Allopurinol[c]		15.5 ± 0.01

[a] The IC$_{50}$ values are presented as the mean ± SD.
[b] Not determined.
[c] Positive control.

Conclusion

In this study, nine compounds were isolated and identified from the fruits of Thai *A. bilimbi* L., including one steroid (**1**), one triterpenoid (**2**), two chalcones (**3** and **4**), two flavonoids (**5** and **6**), one flavonolignan (**7**), and two lignans (**8**-**9**). Among these, compounds **3** and **4** showed the most potent α-glucosidase inhibition (IC$_{50}$ 4.10 ± 0.20 and 4.79 ± 0.27 μM, respectively), while compound **4** displayed the highest XO inhibition (IC$_{50}$ 48.4 ± 0.03 μM). To the best of our knowledge, this is the first report of the isolation of **2**-**4** and **7**-**9** from this plant. These results highlight the importance of further exploring *A. bilimbi* L. Additional research is needed to fully understand the potential of its compounds, particularly for their possible applications in treating diabetes and gout.

Conflict of Interest

The authors declare no conflict of interest.

Authors' Declaration

The authors hereby declare that the work presented in this article is original and that any liability for claims relating to the content of this article will be borne by them.

Acknowledgement

The authors gratefully acknowledge the financial support provided by Faculty of Science and Technology, Thammasat University, Contract No. SciGR 14/2567.

© 2025 the authors. This work is licensed under the Creative Commons Attribution 4.0 International License

References

1. Alhassan AM, Ahmed QU. *Averrhoa bilimbi* Linn.: A review of its ethnomedicinal uses, phytochemistry, and pharmacology. J Pharm Bioallied Sci. 2016; 8(4): 265–271.
2. Prastiyanto ME, Wardoyo FA, Wilson W, Darmawati S. Antibacterial activity of various extracts of *Averrhoa bilimbi* against multidrug-resistant bacteria. Biosaintifika. 2020; 12(2): 163–168.
3. Kumar KA, Gousia SK, Anupama M, Latha JNL. A review on phytochemical constituents and biological assays of *Averrhoa bilimbi*. Int J Pharm Pharm Sci Res. 2013; 3(4): 136–139.
4. Garg M, Chaudhary SK, Kumari S, Goyal A. Phytochemical, biological, and traditional claims on *Averrhoa bilimbi*: An overview. Indian J Pharm Sci. 2022; 84(3): 532–542.
5. Ahmed QU, Alhassan AM, Khatib A, Shah SAA, Hasan MM, Sarian MN. Antiradical and xanthine oxidase inhibitory activity evaluations of *Averrhoa bilimbi* L. leaves and tentative identification of bioactive constituents through LC-QTOF-MS/MS and molecular docking approach. Antioxidants. 2018; 7(10): 137.
6. Miraj AJ, Kabir A, Mamun Y, Akhter S, Ahammed MS, Sultana S, et al. Evaluation of the analgesic and anti-inflammatory activities of methanolic extracts of the leaves of *Averrhoa bilimbi*. Discov Phytomed. 2019; 6(1): 12.
7. Santi TD, Siregar TN, Sutriana A, Andini R, Candra A. Wound healing activity of transdermal patches of *Carica papaya*, *Chromolaena odorata*, and *Averrhoa bilimbi* leaves on incision wounds of hyperglycemic rats. Trends Sci. 2023; 20(12): 6944.
8. Sarker MAM, Chowdhury ASFU. Analgesic effect of methanolic extracts of leaf, bark, and fruit of *Averrhoa bilimbi* Linn. Bangladesh Med Res Counc Bull. 2022; 48(2): 120–126.
9. Meilina R, Suwarso EDY, Dalimunthe A. Relaxation effect of ethanolic extract of *Averrhoa bilimbi* L. leaves on ileum smooth muscle contraction of *in vitro* isolated rat (*Rattus norvegicus*). Asian J Pharm Clin Res. 2018; 11:135–137.
10. Prabhu R, Fernandes R, Govinda KA. Phytoconstituents isolation and hepatoprotective activity potential of *Averrhoa bilimbi* leaf extract. J Pharm Res Int. 2021; 33(58B): 573–581.
11. Bipat R, Toelsie JR, Joemmanbaks RF, Gummels JM, Klaverweide J, Jhanjan N, et al. Effects of plants popularly used against hypertension on norepinephrine-stimulated guinea pig atria. Pharmacogn Mag. 2008; 4(13): 12.
12. Nair MS, Soren K, Singh V, Boro B. Anticancer activity of fruit and leaf extracts of *Averrhoa bilimbi* on MCF-7 human breast cancer cell lines: A preliminary study. Austin J Pharmacol Ther. 2016; 4(2): 1082.
13. Hoang LTTT, Dong PSN, Nguyen VK, Thao VTM, Ramadhan R, Jutakanoke R, Sichaem J. *β*-amyrin heptadecanoate, a new oleanane triterpenoid with *α*-glucosidase inhibitory and cytotoxic activities from the leaves of *Averrhoa bilimbi* L. Nat Prod Res. 2024. Doi: 10.1080/14786419.2024.2425045
14. Azeem AK, Vrushabendraswami BM. Hypolipidemic evaluation of *Averrhoa bilimbi* leaf ethanolic extracts on streptozotocin-induced diabetic rats. J Innov Pharm Biol Sci. 2015; 2(4): 649–652.
15. Gunawan C, Cordero A, Paano A. Structure elucidation of two new phytol derivatives, a new phenolic compound, and other metabolites of *Averrhoa bilimbi*. Res Congr. 2013 Mar; 7–9.
16. Auw L, Subehan, Sukrasno, Kadota S, Tezuka Y. Constituents of Indonesian medicinal plant *Averrhoa bilimbi* and their cytochrome P450 3A4 and 2D6 inhibitory activities. Nat Prod Commun. 2015; 10(1): 57–62.
17. Rohman F, Putra WE, Sustiprijatno, Widiastuti D. Virtual assessment of *Imperata cylindrica* roots bioactive compounds as a potential inhibitor for alpha-glucosidase: The study of Tengger tribe's medicinal plant. Trop J Nat Prod Res. 2021; 5(7): 1240–1245.
18. Osiako FH, Samuel BB, Oluyemi WM. Effects of selected *Terminalia* and *Ficus* species in the inhibition of *α*-amylase and *α*-glucosidase enzymes. Trop J Nat Prod Res. 2023; 7(8): 3775–3780.
19. Li Z, Wang H, Sun S, Shao Z, Lv C, Dong X, Wang W. Ellagitannins from pomegranate (*Punica granatum* L.) flower with xanthine oxidase and *α*-glucosidase inhibitory activities. J Funct Foods. 2024; 116: 106153.
20. Wang H, Zhou X, Liu Y, Xie W, Yang D, Huo D, Wang R. Identification and molecular docking of xanthine oxidase and *α*-glucosidase inhibitors in *Opuntia ficus-indica* fruit. J Food Sci. 2024; 89(7): 4192–4204.
21. Rattanapan J, Sichaem J, Tip-pyang S. Chemical constituents and antioxidant activity from the stems of *Alyxia reinwardtii*. Rec Nat Prod. 2012; 6(3): 288–291.
22. Sichaem J, Aree T, Lugsanangarm K, Tip-Pyang S. Identification of highly potent *α*-glucosidase inhibitory and antioxidant constituents from *Zizyphus rugosa* bark: Enzyme kinetic and molecular docking studies with active metabolites. Pharm Biol. 2017; 55(1): 1436–1441.
23. Hang DTT, Trang DT, Dung DT, Yen DTH, Hoang NH, Bang NA, Cuc NT, Nhiem NX, Huong PTT, Tai BH, Kiem PV. Guaianolide sesquiterpenes and benzoate esters from the aerial parts of *Siegesbeckia orientalis* L. and their xanthine oxidase inhibitory activity. Phytochemistry 2021; 190: 112889.
24. Chaturvedula VSP, Prakash I. Isolation of stigmasterol and *β*-sitosterol from the dichloromethane extract of *Rubus suavissimus*. Int Curr Pharm J. 2012; 1(9): 239–242.
25. Yosioka I, Nakanishi T, Yamauchi H, Kitagawa I. Revised structure of zeorin and its correlation with leucotylin. Tetrahedron Lett. 1971; 12(16): 1161–1164.
26. Ichino K, Tanaka H, Ito K, Tanaka T, Mizuno M. Synthesis of helilandin B, pashanone, and their isomers. J Nat Prod. 1988; 51(5): 906–914.
27. Lien TP, Porzel A, Schmidt J, Van Sung T, Adam G. Chalconoids from *Fissistigma bracteolatum*. Phytochemistry. 2000; 53(8): 991–995.
28. Banerjee C, Nandy S, Chakraborty J, Kumar D. Myricitrin–a flavonoid isolated from the Indian olive tree (*Elaeocarpus floribundus*)–inhibits Monoamine oxidase in the brain and elevates striatal dopamine levels: therapeutic implications against Parkinson's disease. Food Funct. 2022; 13(12): 6545–6559.
29. Sinha R, Gadhwal MK, Joshi UJ, Srivastava S, Govil G. Modifying effect of quercetin on model biomembranes: studied by molecular dynamic simulation, DSC and NMR. Int J Curr Pharm Res. 2012; 4(1): 70–79.
30. Resende FO, Rodrigues-Filho E, Luftmann H, Petereit F, Mello JC. Phenylpropanoid substituted flavan-3-ols from *Trichilia catigua* and their *in vitro* antioxidative activity. J Braz Chem Soc. 2011; 22: 2087–2093.
31. Gohari AR, Saeidnia S, Bayati-Moghadam M, Amin G. Lignans and neolignans from *Stelleropsis antoninae*. Daru. 2011; 19(1): 74.
32. Wang Z, Zhang L, Sun Y. Semipreparative separation and determination of eleutheroside E in *Acanthopanax giraldii* Harms by high-performance liquid chromatography. J Chromatogr Sci. 2005; 43(5): 249–252.
33. Cai CY, Rao L, Rao Y, Guo JX, Xiao ZZ, Cao JY, Wang B. Analogues of xanthones—Chalcones and bis-chalcones as *α*-glucosidase inhibitors and anti-diabetes candidates. Eur J Med Chem. 2017; 130: 51–59.
34. Tran TD, Tu VL, Hoang TM, Dat TV, Tam DNH, Phat NT, Hung DT, Huynh HH, Do TC, Le HH, Minh LHN. A review of the *in vitro* inhibition of *α*-amylase and *α*-glucosidase by chalcone derivatives. Cureus. 2023; 15(4): e37267.
35. Kuroda M, Iwabuchi K, Usui S, Akiyama N, Mimaki Y. Chemical compounds from the leaves of *Verbascum thapsus* and their xanthine oxidase inhibitory activity. Shoyakugaku Zasshi. 2017; 71(1): 49–50.
36. Alizadeh N, Eskandani M, Tondro K, Rashidi MR, Nazemiyeh H. Inhibitory effects of flavonolignans from *Silybum marianum* (L.) Gaertn (milk thistle) on function of aldehyde oxidase and xanthine oxidase in rats. Lett Drug Des Discov. 2018; 15(3): 256–262.

© 2025 the authors. This work is licensed under the Creative Commons Attribution 4.0 International License